

Magneto-Mechanical MEMS Sensors for Bio-Detection

M. Ramasamy, C. Liang and B.C. Prorok
Auburn University, Department of Mechanical Engineering
275 Wilmore Labs, Auburn University, AL 36849-5341
Email: prorok@auburn.edu

ABSTRACT: Ferromagnetic materials have shown to possess some unique and useful properties, one of which is that they are magnetomechanical transducers, that is, they exhibit a change in dimension when they are subjected to an external magnetic field and vice versa. This magneto-mechanical coupling enables magnetoelastic sensors to be driven to resonance via a modulated magnetic field to detect biological species via frequency shift by mass addition [1,2]. This work details the development of an algorithm to predict the number of captured *E. coli* cells based only upon the resonance frequency shift. This is an important issue as attaching cells influence resonance based upon their location on the sensor. It is therefore necessary to develop a statistical protocol to predict the concentration of the target agent present. A protocol was developed based upon data from microscale resonators using polystyrene beads as a simulant. The protocol was verified with numerical studies and experiments using *E. coli* cells.

INTRODUCTION: Food safety has become an important issue in the past decade after numerous intentional and unintentional contaminations. With the innovation in science and technology, there has been a remarkable increase in the development of biological weapons throughout the world. Biological agents are considered to be psychologically threatening and therefore provide more appeal to the terrorist. The human pathogenic limit of many engineered biological agents have been reduced in order of magnitude from 10^{15} to few cells [3]. This has led to more research on developing biological agents' detection techniques that are very rapid, sensitive and cost effective [4]. Magnetostrictive materials developed into mass-based acoustic wave Sensor operated on longitudinal vibration mode is one such technique. Magnetostrictive materials are soft amorphous ferromagnetic materials that change in magnetic properties when stress is applied or vice versa. These magnetostrictive materials are fashioned into acoustic wave sensors in the form of simple rectangular strips that are actuated in their longitudinal vibration mode when exposed to magnetic field. Due to the applied field the strips resonate at a specific frequency which is dependent on their mass and physical dimensions [1-4]. These devices operate similar to magnetostrictive strips used in stores as a surveillance device to prevent the theft of goods.

PRINCIPLE OF OPERATION

In this research, the principle of detection of these sensors involved measuring a resonant frequency shift as the target biological species attaches to the sensor; effectively this addition of mass dampens the resonant behavior of the sensor platform [10]. In the case of monitoring harmful biological agents, it is highly desired to detect the presence of a handful of spores/cells since many harmful agents have a very low pathogenic limit in humans, meaning it only takes a few spores/cells to infect them. When biological agents attach to these magnetostrictive sensors in small amounts they represent discrete mass additions, whereas a large number may be more analogous to mass evenly distributed on the strip. It is therefore highly desirable to better understand how spore/cell attachment location influences the resonant frequency of these magnetostrictive strips.

The basic sensor structure investigated was a freestanding beam with no fixed ends. The resonance frequency of the first harmonic mode of such a structure can be described as

$$f = \frac{1}{2L} \sqrt{\frac{E}{\rho(1-\nu)}} \quad (1)$$

Where, L , E , and ρ are the length, Young's modulus, and density of the sensor strip, respectively. As these freestanding magnetostrictive strips are driven to their first harmonic mode, the entire strip deforms in response to the field. The resulting deformation waves propagate through the strip and reflect back from the free ends and cancel at the strip's center, which is the zero nodal position for a freestanding beam resonating in its first

harmonic mode [17]. It should be noted that positions further from the center node of the strip move further from the node during deformation due to the accumulated deformations of all positions between it and the node. Thus, the free ends move the furthest which is clearly seen in [figure1a](#) portraying the simulation result of a mass sensor developed using Ansys® as the simulation tool. Variation in the shade from black to light shade of gray depicts the level of deformation experienced by the sensor platform due to the longitudinal vibration following the boundary conditions.

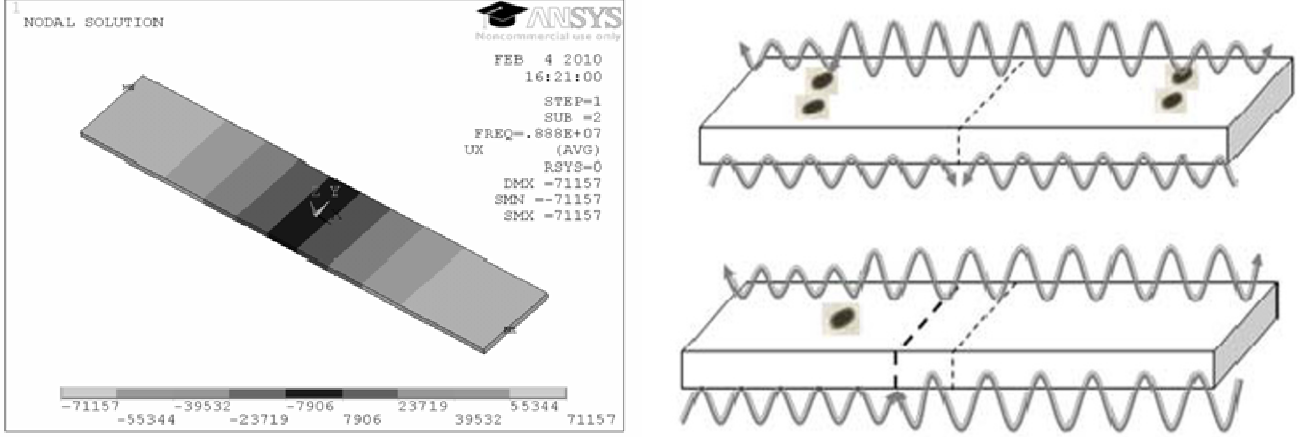


Figure 1: Deformation of Longitudinally vibrated Sensor and Mass attachment affection the wave speed of the platform

When mass becomes attached to the sensor it effectively dampens the speed of the deformation waves propagating in the strip, which reduces its resonant frequency. [Figure1b](#) represents the action of deformation waves due to the mass attachment. In the first case *E. coli* cells are attached to the sensor platform at equal distance from the nodal point [12-16]. The deformation waves subjected to this mass travel with reduced wave speed from that point and reach the central nodal position leading to the resonant frequency shift. Whereas in the second case mass is attached on one side of the sensor leading to shift in the nodal point to balance for the reduced wave speed on one side alone and hence we observe a resonant frequency shift. This paper elaborately discusses detection of biological agent considering the above cases, on the acoustic response of the sensor [11]. The frequency shift as a result of mass attachment for acoustic-based sensors such as these is described the following equation,

$$\Delta f = -f_o \left\{ \frac{\eta}{2} \right\}. \quad (2)$$

Where $\eta = \Delta m / m_{sen}$ and Δm is the mass bonded on a sensor, Δf is the resonant frequency change before and after mass attachment, m_o and f_o is the sensor's initial mass and resonant frequency, respectively [2-4]. Here, the bonded mass (Δm) on the sensor's surface is considered as an evenly distributed mass and is considerably small with respect to the sensor's mass. Accordingly, the change in frequency can be related to the amount of mass bonded on the sensor [8]. However, in the case when a mass is not evenly distributed or is a discrete mass bonded in a particular location this equation is no longer valid. In order to study these effects discrete masses were attached at various positions on the sensor and the response was measured and analyzed. For experimental analysis a schematic setup as shown in [figure 2](#) involving a coil, external magnetic bias and a network analyzer was used to measure the acoustic response of the sensor as discussed in

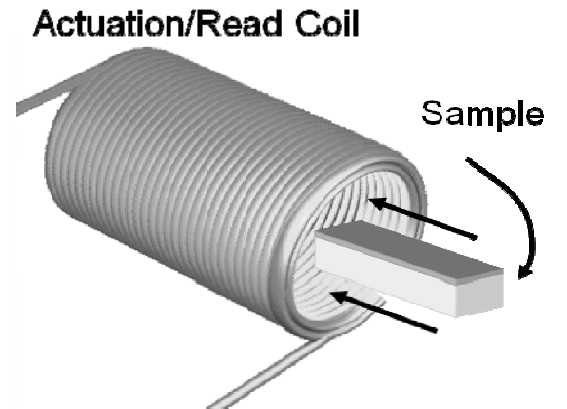


Figure 2: Schematic representation of the measurement rig.

previous work by the authors [1-3]

DESIGN AND EXPERIMENTAL METHODS:

Numerical simulations were carried out using commercially available software Ansys®. Specifically, the simulations involved modal analysis on an undamped, freestanding beam with oscillations in the longitudinal mode both with and without attached mass. The structural physical (engineering) discipline is preferred for the Modal analysis of Magnetostrictive sensors. The selected element type was SOLID186. The sensor size employed here was $250 \times 50 \times 4 \mu\text{m}$ and the attached mass were representative of an actual *E. Coli* O157:H7 cell, size of $1.43 \times 0.73 \times 0.73$ microns and weight of 1 pictogram. The boundary conditions were set to obtain longitudinal vibration mode of the sensor platform. Prediction model was developed involving the factors influencing the resonance behavior such as (a) Mass distribution, (b) Position of the mass distributed and (c) Physical dimension of the sensor platform in compliance with the theoretical equations and simulation results. Mass of *E. coli* cells were distributed as a single layer for uniform distribution. The later was glued to the sensor platform and subjected to numerical simulation with the application of boundary condition over the whole setup. The density of the layer was modified each time for different amount of mass in uniform distribution case and the corresponding variation in frequency shift was observed. In case of the non uniform distribution the layer was split and concentrated along the free ends gradually moving towards the central nodal line and vice versa as shown in Figure 3. The darker layer in the figure is considered as the mass of *E. coli* cell distributed over the sensor platform.

Glass beads attachment : Sensors with dimensions of 5 mm length and 1 mm width were cut from a $28 \mu\text{m}$ thick commercially available Metglas™ 2826MB strip. These specimens were prepared, by cleaning and drying, using the identical procedures described by the authors elsewhere. Glass beads with a diameter about $425 \mu\text{m}$ were employed to simulate the concentrated mass and were carefully loaded on to the sensor surface at prescribed locations and secured with adhesive. The average mass of a sensor and glass bead were $1066 \mu\text{g}$ and $181.5 \mu\text{g}$, respectively. It should be noted that these experiments are aimed as assessing the position of the mass concentrations and not focused on demonstrating minimum sensitivity. Thus, significantly sized beads were employed. The amount of glue employed to affix each bead as well as its position were well controlled to minimize any errors. After a glass bead was loaded on the sensor surface, it was immobilized by drying at

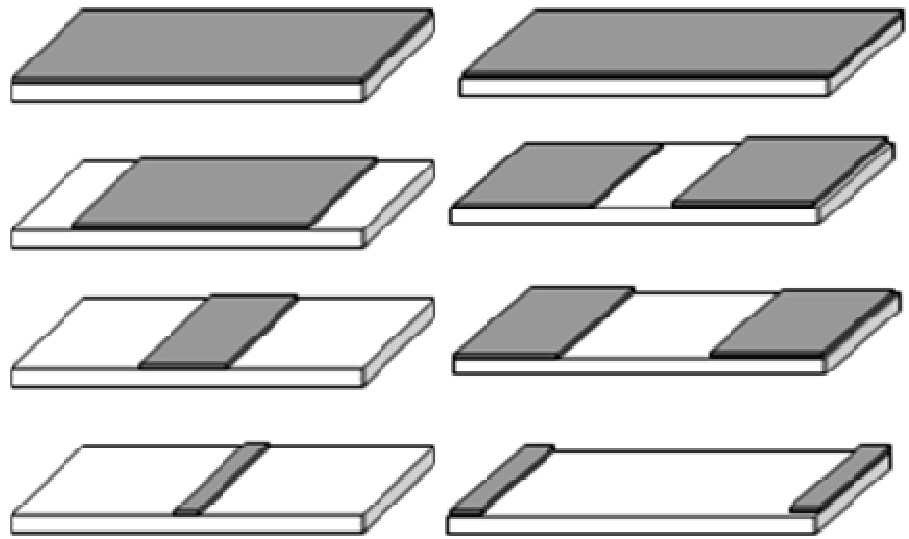


Figure 1: Non-Uniform distribution of *E. coli* cells as layer over the sensor

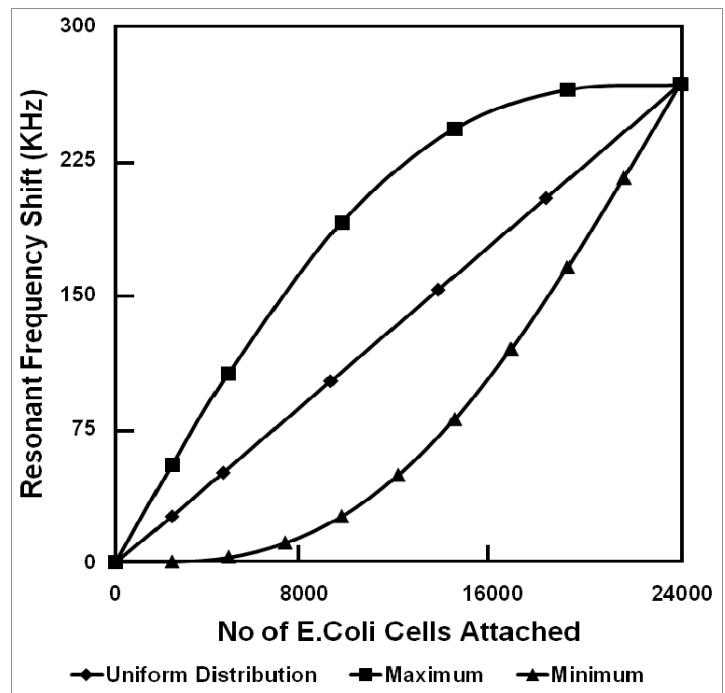


Figure 2: Simulation result of resonant frequency shift due to *E. coli* cells distribution

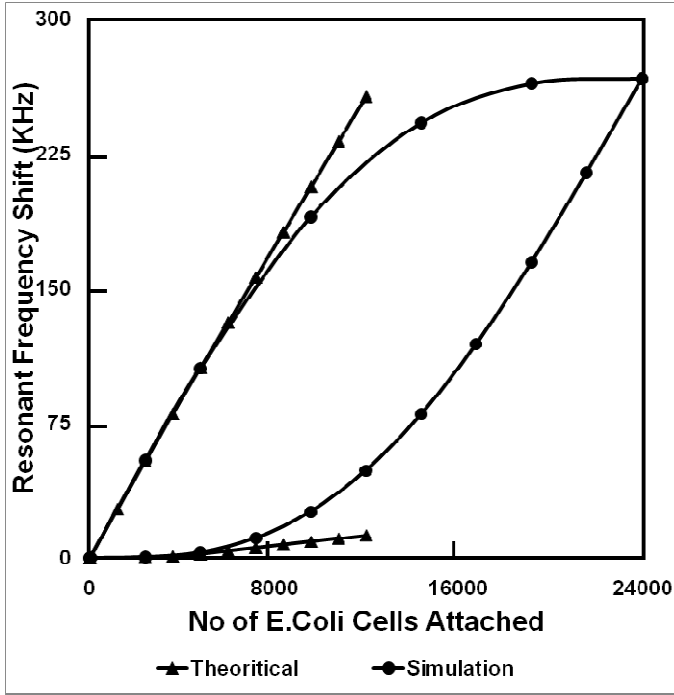


Figure 5: comparative plot of resonant Frequency shift in theoretical and simulated study.

demonstrated by Guntupalli, et al. and Wan, et al. in their experimental analysis. In such cases the Maximum resonant frequency shift will be observed at the free ends of the sensor platform which can theoretically determined using equation.

$$\Delta f = -f_o \left\{ \left(\frac{KL}{2\pi} \right) - 1 \right\}. \quad (3)$$

Where $K = \beta \sqrt{\frac{\rho}{E}}$, and β is the angular frequency and using η we can calculate KL value for a free standing beam using the equation,

$$\eta(KL) = \tan(KL)$$

Mathematically speaking the frequency shift for certain amount of mass will have a tolerance limit based on their location and distribution. From the above equation we know that the maximum frequency shift for certain amount of mass is observed at the free ends of the sensor platform. This eventually explains the fact that the minimum frequency shift for the same amount of mass would be observed when concentrated at the centre. When mass is distributed close to the nodal point since the deformation experienced is relatively lower compared to the free ends, we observe minimum frequency shift close the centerline of the sensor platform.

room temperature for at least two hours. The resonant frequency of the sensor was measured before and after attachment of the glass bead in a manner identical to which is discussed in previous work by the authors.

RESULT AND DISCUSSION

(a) Resonant Frequency shift due to Mass Distribution: Frequency shift is not the same if the mass is concentrated at a particular location on the sensor platform compared to the uniform distribution of the mass. This is mainly due to reduction in wave speed of the sensor obstructed by the concentrated mass at discrete locations on the platform. Simulation results are shown in the figure 4. From the figure we can notice that uniform distribution shows a linear plot with the increase in frequency shift as the amount of mass increases gradually. The upper and lower plot in the figure explains the distribution of mass as layer as shown in figure 3 from free end to the central nodal point and vice versa. In these 2 cases the plots meet the uniform distribution linear plot at the end since that's the maximum possible mass that could be attached over the sensor platform. This mass number is based on the assumption that no two E. coli cells accumulate one over the other as

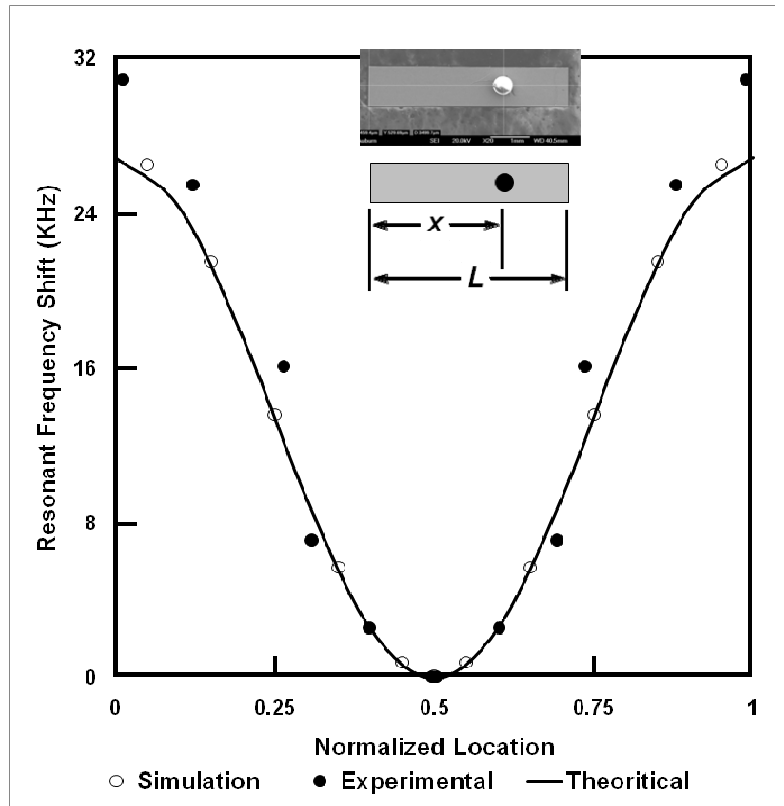


Figure 6: Position sensitive Resonant Frequency shift due to Mass attachment

$$\Delta f = -f_o \left\{ \eta + \left(\frac{KL}{2\pi} \right) - 1 \right\}. \quad (4)$$

We were able to formulate an equation for minimum frequency shift due to concentration of mass along the centerline of the sensor platform. These equations were verified with the help of the simulation results obtained by distributing the mass uniformly and at various discrete positions on the sensor platform as shown in Figure 5. From the figure we can also notice that after a certain amount of the mass the movement of the theoretical plot deviate in a linear manner compared to the simulation plot which is mainly due to the assumption made in accordance to the distribution of load along the free ends. but in reality as the mass increases it moves closer to the nodal point and eventually meet the uniform distribution line at a particular amount of mass which is the same in case of minimum frequency shift of the sensor due to mass distribution.

(b) Influence of position: Tolerance limit of frequency shift depends on the position of the mass attached irrespective of the amount of mass involved. In this case, the wave speed on the side of the attached mass is less than the opposite side where no mass is attached. During resonance, the wave frequency must match on either side of the sensor. In order to account for the imbalance of wave speeds, the zero nodal point must shift such that the distance the waves travel on each side enables the waves to arrive at the nodal point at the same time to ensure they are in phase. In this case it must shift towards the side with the attached mass, resulting in larger frequency shifts. The simulation and experimental results using glass beads that were attached to the sensor proves this conception. Using these results an equation was developed, to represent the influence of position on the frequency shift of the sensor.

$$\Delta f = \frac{-f_o}{2} \left(\frac{\Delta m}{m_{sen}} \right) \left\{ 1 - \cos \left(\frac{\pi x}{L} \right) \right\} \quad (5)$$

In this case, where the attached mass is a discrete mass bonded in a particular location, the wave speed on the side of the attached mass is less than the opposite side where no mass is attached. During resonance, the wave frequency must match on either side of the sensor. In order to account for the imbalance of wave speeds, the zero nodal point must shift such that the distance the waves travel on each side enables the waves to arrive at the nodal point at the same time to ensure they are in phase. In this case it must shift towards the side with the

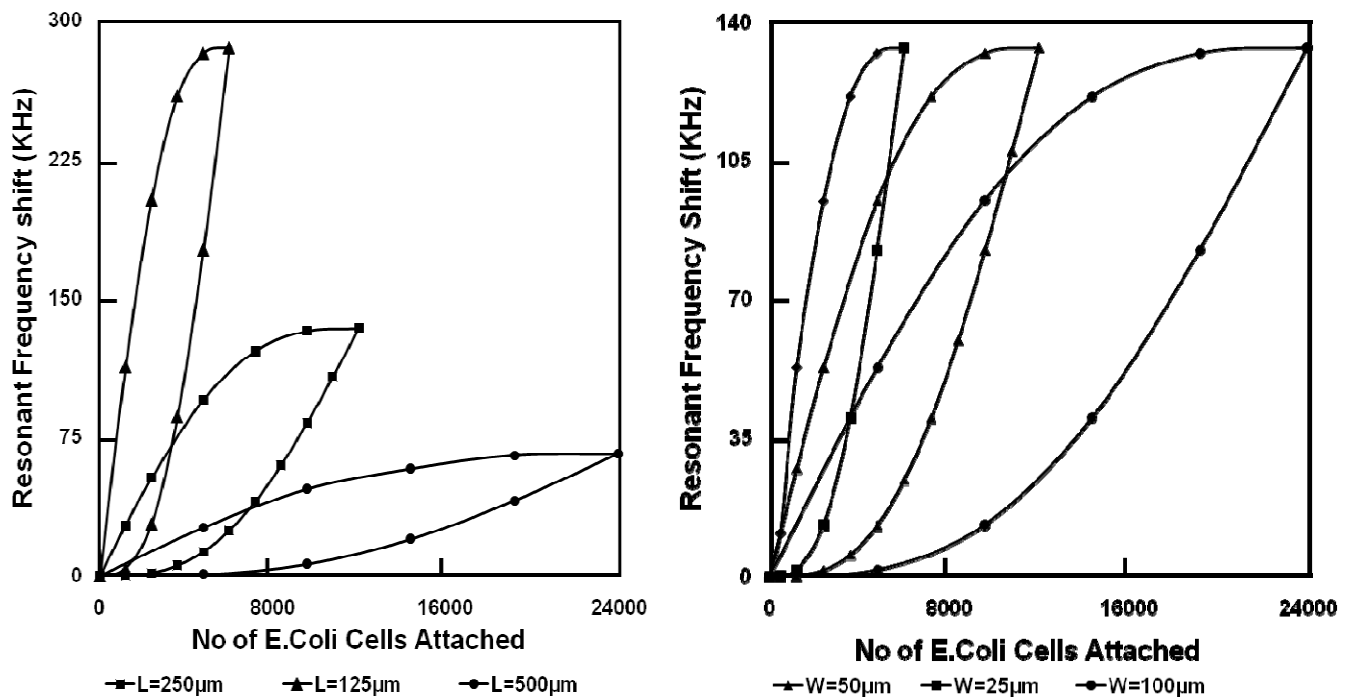


Figure 7: Plot illustrating the influence of physical dimension on the resonant frequency shift of the sensor platform

attached mass. Thus, as the mass is moved further away from the original nodal point, the wave speeds are increasingly imbalanced and the node must shift further to account for it, resulting in larger frequency shifts.

Beads were also positioned away from the longitudinal center axis of the sensor to assess the influence of lateral position for the same longitudinal position x . The frequency shift was relatively unaffected indicating that lateral positioning for a discrete mass addition was negligible in comparison to longitudinal positioning.

(c) Influence of dimensions on resonant frequency shift: Simulations were carried out to study the effect of variation in resonance behavior due to change in dimensions of the sensor. Figure 5(a) shows that variation in length of the sensor has a dramatic effect on the frequency shift. When the sensor is subjected to Longitudinal vibration, due to the sensor materials magnetic property the deformation occurs in the longitudinal direction along the direction of the applied field. The larger the length of the sensor greater is the sensitivity and hence greater resonant frequency shift for the same amount of mass. In figure 5(b) variation in width of the sensor platform does not have any influence on the acoustic response of the sensor. This is because lateral axis of the sensor does not experience any deformation due to their restricted boundary conditions and hence distribution of mass is considered to uniform along the lateral distance at any point on the sensor platform. This is experimentally proved with the help of polystyrene glass beads that had no influence on the resonant frequency shift when attached along their lateral position of the sensor platform.

CONCLUSION

A Model developed based on the acoustic response of Magnetostrictive Sensor actuated longitudinally with the modulated magnetic field. Numerical simulations and experimental verifications were carried out with the predicted model considering the factors influencing the resonance behavior of the sensor. The tolerance limit of frequency shift corresponding to the distribution of mass, discrete position of the mass attached and the physical dimensions of the sensor platform were determined in several ways. A Good agreement was found between these results offering a good paradigm for detecting biological agents.

References

- [1] C. Liang and B. C. Prorok, "Measuring the Thin Film Elastic Modulus with a Magnetostrictive Sensor," J. Micromech. Microeng., vol. 17, pp. 709-716, 2007.
- [2] C. Liang, S. Morshed, and B. C. Prorok, "Correction for Longitudinal Mode Vibration in Thin Slender Beams," Appl. Phys. Lett., vol. 90, pp. 221912, 2007.
- [3] M. L. Johnson, J. Wan and B. A. Chin et al., "A Wireless Biosensor using Microfabricated Phage-Interfaced Magnetoelastic Properties", Sens. Act. A 144, 38-47, 2008.
- [4] W. Shen, R.S. Lakshmanan and B.A. Chin et al., "Phage Coated Magnetoelastic Micro-Biosensors for real-time Detection of B.anthraxis spores", Sens. Act. B 137, pp.501-506, 2009.
- [5] D. S. Ballantine, R. M. White, S. J. Martin, A. J. Rico, G. C. Frye, E. T. Zellers, and H. Wohltjen, Acoustic Wave Sensors: Theory, Design, and Physical-chemical applications. New York: Academic Press, 1997.
- [6] R. Raiteri, M. Grattarola, H. J. Butt, and P. Skladal, "Micromechanical cantilever-based biosensors," Sens. Act. B, vol. 79, pp. 115, 2001.
- [7] P. G. Stoyanov, S. A. Doherty, C. A. Grimes, and W. R. Seitz, "A remotely interrogatable sensor for chemical monitoring," IEEE Trans. Mag., vol. 34, pp. 1315, 1998.
- [8] C. Mungle, C. A. Grimes, and W. R. Dreschel, "Magnetic field tuning of the frequency-temperature response of a magnetoelastic sensor," Sens. Act. A, vol. 101, pp. 143, 2002.
- [9] C. Ruan, K. Zeng, O. K. Varghese, and C. A. Grimes, "A staphylococcal enterotoxin B magnetoelastic immunosensor," Biosens. Bioelec., vol. 20, pp. 585, 2004.
- [10] N. Bouropoulos, D. Kouzoudis, and C. A. Grimes, "The real-time, in situ monitoring of calcium oxalate and brushite precipitation using magnetoelastic sensors," Sens. Act. B, vol. 109, pp. 227, 2005.
- [11] S. Schmidt and C. A. Grimes, "Characterization of nano-dimensional thin-film elastic moduli using magnetoelastic sensors," Sens. Act. A, vol. 94, pp. 189, 2001.
- [12] L. S.Q., L. Orona, Z. M. Li, and Z.-Y. Cheng, "Biosensor Based on Magnetostrictive Microcantilevers as a Sensor Platform," Appl. Phys. Lett., vol. 88, pp. 073507, 2006.

- [13] J. Wan, H. Shu, S. Huang, B. Fiebor, I.-H. Chen, V. A. Petrenko, and B. A. Chin, " Phage-Based Magnetoelastic Wireless Biosensors for Detecting Bacillus Anthracis Spores," IEEE Sens. J., vol. 7, pp. 470-477, 2007.
- [14] T. Thundat, E. A. Wachter, S. L. Sharp, and R. J. Warmack, "Detection of mercury vapor using resonating microcantilevers," Appl. Phys. Lett., vol. 66, pp. 1695, 1995.
- [15] G. Y. Chen, R. J. Warmack, T. Thundat, D. P. Allison, and A. Huang, "Resonance response of scanning force microscopy cantilevers," Rev. Sci. Instr., vol. 65, pp. 2532, 1994.
- [16] B. Ilic, D. Czaplewski, M. Zalalutdinov, C. H.G., P. Neuzil, C. Campagnolo, and C. Batt, "Single cell detection with micromechanical oscillators," J. Vac. Sci. Tech. B, vol. 19, pp. 2825, 2001.
- [17] R. D. Blevins, Formulas for natural frequency and mode shape. Malabar, FL. USA: Krieger Publishing Company, 2001. M. D. Ward and D. A. Buttry, "Insitu Interfacial Mass Detection with Piezoelectric Transducers," Science, vol. 249, pp. 1000, 1990.

MEMS and Nanotechnology, Volume 2
Proceedings of the 2010 Annual Conference on
Experimental and Applied Mechanics
Proulx, T. (Ed.)
2011, X, 282 p., Hardcover
ISBN: 978-1-4419-8824-9